Nucleon momentum distributions in ^{3}He and three-body interactions

S.V. Bekh*

National Technical University of Ukraine "Igor Sikorsky Kyiv Polytechnic Institute"

Prospect Peremogy 37, 03056 Kiev, Ukraine

A.P. Kobushkin†

Bogolyubov Institute for Theoretical Physics,

Nat. Acad. of Sci. of Ukraine

14b, Metrolohicheskaya Str.,

Kiev 03143, Ukraine

and

National Technical University of Ukraine "Igor Sikorsky Kyiv Polytechnic Institute"

Prospect Peremogy 37, 03056 Kiev, Ukraine

E.A. Strokovsky‡

Laboratory of High Energy Physics,

Joint Institute for Nuclear Research

141980, Dubna, Russia and

Research Center for Nuclear Physics, Osaka University

10-1 Mihogaoka, Ibaraki Osaka, 567-0047, Japan

arXiv:1704.07662v1 [nucl-th] 25 Apr 2017

Abstract

We calculate momentum distributions of neutrons and protons in ^{3}He in the framework of a model which includes 3N interactions together with 2N interactions. It is shown that contribution of 3N interactions becomes essential in comparison with contribution coming from 2N interaction for internal momentum in ^{3}He $k > 250$ MeV/c. We also compare calculated momentum distribution of protons with so-called empirical momentum distribution of protons extracted from A(^{3}He, p) breakup cross-sections measured for protons emitted at zero degree. It is concluded that 3N interactions cannot completely explain the disagreement between the available data on the empirical momentum distribution of protons in ^{3}He and calculations based on 2N interaction, which is observed at high momentum region of the momentum distribution, $k > 250$ MeV/c.

PACS numbers:

*Electronic address: bekh@bitp.kiev.ua

†Electronic address: kobushkin@bitp.kiev.ua

‡Electronic address: strok@jinr.ru

I. INTRODUCTION

Momentum distributions of nucleons in nuclei are directly connected with the spatial structure of the corresponding nuclear systems. In particular, these distributions at Fermi momenta above 200-300 MeV/c (this region is usually referred to as "a region of high relative nucleon momenta") give important information about such interesting questions as a role of non-nucleon degrees of freedom in nuclear structure, relativistic effects, and so on.

Starting from three nucleon systems, ^{3}He and ^{3}H, the momentum distributions should also give information about the role of effective three-nucleon (3N) interactions in nuclear structure.

The goals of this paper are:

1. to find signals of manifestation of 3N interactions in the momentum distributions of neutrons and protons in ^{3}He,

2. to compare theoretical results, coming for known models for 2N+3N interactions, with existing experimental data,

3. to indicate what region of relative nuclear momenta should be looked for manifestations of non-nucleon degrees of freedom in nuclear structure.

The paper is organized in the following way. We start, in Sect. II, with a short overview of an operator form of three nucleon bound state, which is a basic point for further calculations. In Sec. III the momentum distribution of neutrons in ^{3}He is calculated within a model, which takes into account 3N interaction together with the standard 2N interaction. In Sec. IV the momentum distribution of protons in ^{3}He is calculated in the framework of the similar model. The calculated proton momentum distribution is compared with existing experimental data in Sec. V, namely: in Subsec. V A we discuss definition and a procedure of extraction of the so called "empirical momentum distribution" of protons in ^{3}He from A(^{3}He, p) breakup cross-sections [1], when the proton-spectator was emitted at 0°; in Subsec. V B the empirical momentum distribution is compared with results of our calculations, as well as with calculations without explicit inclusion of the 3N interaction. Conclusions are given in Sec. VI.

II. OPERATOR FORM OF THREE NUCLEON BOUND STATE

There are few known approaches to describe a three nucleon (3N) wave function: a partial wave decomposition (see, e.g., Ref. [2]), tensor representations [3–5], and the operator form [6]. In this paper we use the last one.

In 1942 E. Gerjouy and J. Schwinger introduced an operator form for three and four nucleon states [6], which was a generalization of an operator form of the deuteron state elaborated earlier by Rarita and Schwinger [7]. In the case of a 3N nucleon state this approach expresses the general spin structure of a 3N system in terms of nine operator forms acting on the special spin state

$$|\nu\rangle = \frac{1}{\sqrt{2}} \left(|+ - \ \ \mathrm{sign}\, \nu\rangle - |- + \ \ \mathrm{sign}\, \nu\rangle \right), \tag{1}$$

where nucleons 1 and 2 have total spin $s = 0$ and the nucleon 3 carries out the spin of the 3N system; ν is the magnetic quantum number of the 3N system. In Eq. (1)

$$|\mathrm{sign}\, m_1 \ \mathrm{sign}\, m_2 \ \mathrm{sign}\, m_3\rangle$$

is a spin wave function of three nucleons with magnetic quantum numbers m_1, m_2, and m_3. The operator form does not employ the isospin formalism and the nucleons are labelled as follows:

$N_1 = N_2 = p$ and $N_3 = n$ — for ^{3}He,
$N_1 = N_2 = n$ and $N_3 = p$ — for ^{3}H.

Relations between approaches which employ or do not employ the isospin formalism, as well as advantages of the latter ones, were discussed in Refs. [8, 9].

It was mentioned in Ref. [10], that the ninth spin structure of the operator form of 3N system is redundant and we, following to Ref. [10], omit this component.

Finally, the 3N bound state wave function is given by

$$\Psi_\nu(\mathbf{p}, \mathbf{q}) = \sum_{i=1}^{8} \phi_i(p, q, x) \, |i, \nu\rangle \,, \tag{2}$$

where $|i, \nu\rangle$ are the spin wave functions defined below (see, Eqs. (4)), $\mathbf{p}$ and $\mathbf{q}$ are the Jacobi

momenta

$$\begin{aligned}
\mathbf{p}_1 &= \tfrac{1}{3}\mathbf{P} - \tfrac{1}{2}\mathbf{q} + \mathbf{p}\,, \\
\mathbf{p}_2 &= \tfrac{1}{3}\mathbf{P} - \tfrac{1}{2}\mathbf{q} - \mathbf{p}\,, \\
\mathbf{p}_3 &= \tfrac{1}{3}\mathbf{P} + \mathbf{q}\,;
\end{aligned} \tag{3}$$

here $\mathbf{p}_1$, $\mathbf{p}_2$, and $\mathbf{p}_3$ are momenta of the nucleons and $\mathbf{P}$ is momentum of the nucleus; $x = \cos\alpha$ (α is angle between the vectors $\mathbf{p}$ and $\mathbf{q}$) and $\phi_i(p,q,x)$ are scalar functions. The scalar functions $\phi_i(p,q,x)$ have been calculated in Ref. [10] for two modern potentials: the 2N potential AV18 [11] with the 3N potential Urbana-IX [12] (AV18+U9) and the 2N potential CD-Bonn [13] with the 3N potential Tucson-Melbourne [14] (CDBN+TM). The functions $\phi_i(p,q,x)$ are tabulated on 3-dimensional grid (x,q,p) and can be downloaded from the site [15].

The spin structures are given as follows:

$$\begin{aligned}
|1\nu\rangle &= |\nu\rangle\,, \\
|2\nu\rangle &= \sqrt{\tfrac{1}{3}}\boldsymbol{\sigma}(12)\cdot\boldsymbol{\sigma}(3)\,|\nu\rangle\,, \\
|3\nu\rangle &= -i\sqrt{\tfrac{3}{2}}\boldsymbol{\sigma}(3)\cdot(\widehat{\mathbf{p}}\times\widehat{\mathbf{q}})\,|\nu\rangle\,, \\
|4\nu\rangle &= \sqrt{\tfrac{1}{2}}\,[i\boldsymbol{\sigma}(12) + \boldsymbol{\sigma}(12)\times\boldsymbol{\sigma}(3)]\cdot(\widehat{\mathbf{p}}\times\widehat{\mathbf{q}}) \\
&\qquad\qquad \times|\nu\rangle\,, \\
|5\nu\rangle &= \left[-i\boldsymbol{\sigma}(12) + \tfrac{1}{2}\boldsymbol{\sigma}(12)\times\boldsymbol{\sigma}(3)\right]\cdot(\widehat{\mathbf{p}}\times\widehat{\mathbf{q}}) \\
&\qquad\qquad \times|\nu\rangle\,, \\
|6\nu\rangle &= \sqrt{\tfrac{3}{2}}\left[\boldsymbol{\sigma}(12)\cdot\widehat{\mathbf{p}}\,\boldsymbol{\sigma}(3)\cdot\widehat{\mathbf{p}} - \tfrac{1}{3}\boldsymbol{\sigma}(12)\cdot\boldsymbol{\sigma}(3)\right] \\
&\qquad\qquad \times|\nu\rangle\,, \\
|7\nu\rangle &= \sqrt{\tfrac{3}{2}}\left[\boldsymbol{\sigma}(12)\cdot\widehat{\mathbf{q}}\,\boldsymbol{\sigma}(3)\cdot\widehat{\mathbf{q}} - \tfrac{1}{3}\boldsymbol{\sigma}(12)\cdot\boldsymbol{\sigma}(3)\right] \\
&\qquad\qquad \times|\nu\rangle\,, \\
|8\nu\rangle &= \tfrac{3}{2\sqrt{5}}\left[\boldsymbol{\sigma}(12)\cdot\widehat{\mathbf{q}}\,\boldsymbol{\sigma}(3)\cdot\widehat{\mathbf{p}}\right. \\
&\quad \left.+\boldsymbol{\sigma}(12)\cdot\widehat{\mathbf{p}}\,\boldsymbol{\sigma}(3)\cdot\widehat{\mathbf{q}} - \tfrac{2}{3}\widehat{\mathbf{p}}\cdot\widehat{\mathbf{q}}\boldsymbol{\sigma}(12)\cdot\boldsymbol{\sigma}(3)\right]|\nu\rangle\,,
\end{aligned} \tag{4}$$

where $\widehat{\mathbf{q}} = \mathbf{q}/|\mathbf{q}|$, $\widehat{\mathbf{p}} = \mathbf{p}/|\mathbf{p}|$, and

$$\boldsymbol{\sigma}(12) = \tfrac{1}{2}[\boldsymbol{\sigma}(1) - \boldsymbol{\sigma}(2)]\,; \tag{5}$$

$\boldsymbol{\sigma}(i)$ are the Pauli matrices of i-th nucleon.

TABLE I: Overlap of the spin structures $\langle i\nu|j\nu\rangle$. Only nonvanishing overlaps are presented.

i j	$\langle i\nu\|j\nu\rangle$	i j	$\langle i\nu\|j\nu\rangle$
1 1	1	6 8	$\sqrt{\frac{6}{5}}x$
2 2	1	7 7	1
6 6	1	7 8	$\sqrt{\frac{6}{5}}x$
6 7	$\frac{1}{2}(3x^2-1)$	8 8	$\frac{9}{10}(1+\frac{1}{3}x^2)$

Normalization of the wave function is given by

$$\int d^3q d^3p \left|\Psi_\nu(\mathbf{p},\mathbf{q})\right|^2 \tag{6}$$

$$= 8\pi^2 \int_{-1}^{1} dx \int_0^\infty dq q^2 \int_0^\infty dp p^2$$

$$\times \left[\sum_{i=1}^{8} \langle i\nu\,|i\nu\rangle\, \phi_i^2(p,q,x) \right. \tag{7}$$

$$\left. + 2\sum_{i\neq j} \langle i\nu\,|j\nu\rangle\, \phi_i(p,q,x)\phi_j(p,q,x) \right] = 1.$$

Overlaps of the spin structures are given in Table I.

Note that contribution of $\phi_3(p,q,x)$, $\phi_4(p,q,x)$, and $\phi_5(p,q,x)$ to the normalization relation 7 is of order of $\sim 0.05\%$ and we will ignore them in the forthcoming calculations.

We have found that numerical calculations, published in Refs [10, 15], are represented on a 3-dimensional grid (p,q,x) which is not "dense" enough for needs of our calculations.

Therefore we expanded the scalar functions $\phi_i(p,q,x)$ at fixed p and q in series in terms

of the Legendre polynomials $P_\ell(x)$:

$$\begin{aligned}
\phi_1(p,q,x) &= C_{10}(p,q) + C_{12}(p,q)P_2(x),\\
\phi_2(p,q,x) &= C_{21}(p,q)P_1(x) + C_{23}(p,q)P_3(x),\\
\phi_3(p,q,x) &= C_{31}(p,q)P_1(x),\\
\phi_4(p,q,x) &= C_{40}(p,q) + C_{42}(p,q)P_2(x),\\
\phi_5(p,q,x) &= C_{50}(p,q) + C_{52}(p,q)P_2(x),\\
\phi_6(p,q,x) &= C_{61}(p,q)P_1(x),\\
\phi_7(p,q,x) &= C_{71}(p,q)P_1(x),\\
\phi_8(p,q,x) &= C_{80}(p,q) + C_{82}(p,q)P_2(x).
\end{aligned} \tag{8}$$

Terms with the Legendre polynomials of higher orders on ℓ were found to be negligibly small and will be omitted in the present numerical calculations.

The coefficients $C_{i,\ell}(p,q)$ of the series, form 13 functions given on a 2-dimensional grid (p,q).

III. MOMENTUM DISTRIBUTION OF NEUTRONS IN ^{3}HE

The momentum distribution of a neutron in ^{3}He is defined as follows (see [10]):

$$\begin{aligned}
n(K) &= \tfrac{1}{2}\sum_\nu \int d^3p d^3q \delta(\mathbf{q}-\mathbf{K}) \left|\Psi_\nu(\mathbf{p},\mathbf{q})\right|^2\\
&= \int d^3p \left|\Psi_{\frac{1}{2}}(\mathbf{p},\mathbf{K})\right|^2,
\end{aligned}$$

$\mathbf{K}$ is the neutron momentum inside ^{3}He. The factor $\frac{1}{2}$ comes from averaging over the nucleus magnetic quantum numbers. Using the spin structures $\langle i\nu|j\nu\rangle$ from Tabl. I, we get

$$n(K) = 2\pi \int_0^\infty p^2 dp \int_{-1}^1 dx\, \Phi(p,K,x), \tag{9}$$

where

$$\begin{aligned}
\Phi(p,K,x) &= \phi_1^2(p,K,x) + \phi_2^2(p,K,x)\\
&+ \phi_6^2(p,K,x) + \phi_7^2(p,K,x)\\
&+ \tfrac{9}{10}\left(1+\tfrac{1}{3}x^2\right)\phi_8^2(p,K,x)\\
&+ \left(-1+3x^2\right)\phi_6(p,K,x)\phi_7(p,K,x)\\
&+ \sqrt{\tfrac{24}{5}}x\left[\phi_6(p,K,x)+\phi_7(p,K,x)\right]\phi_8(p,K,x).
\end{aligned} \tag{10}$$

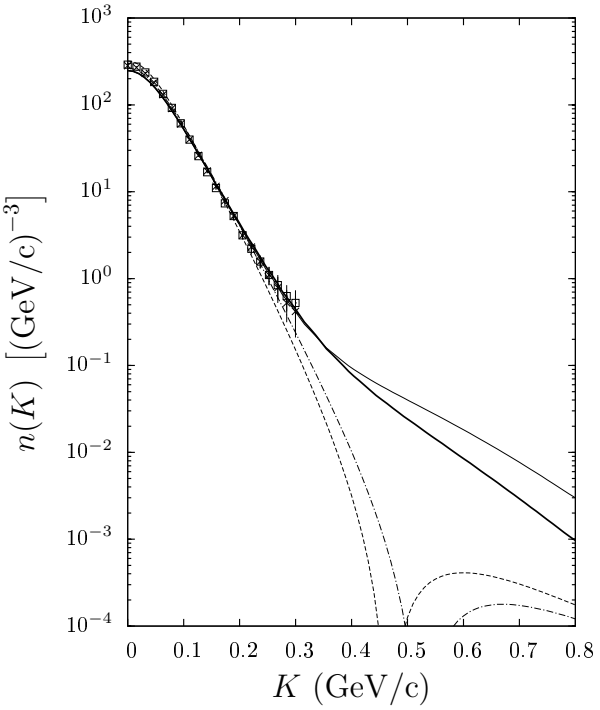

FIG. 1: The momentum distribution of neutrons in ^{3}He calculated with 2N+3N interaction, AV18+U9 (thin solid line) and CDBN+TM (thick solid line). The results obtained with 2N interaction only (dashed and dot-dashed lines, for the Paris [18] and CD-Bonn [13] potentials, respectively) are taken from Ref. [16]. The squares and crosses represent results of variational calculations [17] obtained with the Urbana+U9 and Argonne+U9 interactions, respectively.

The resulting neutron momentum distribution, $n(K)$, for AV18+U9 and CDBN+TM together with results of variational calculations from Ref. [17], are shown in Fig. 1. We compare this result with calculations from Ref. [16] obtained without 3N interactions. Good agreement between the results, obtained with and without 3N interaction, is obvious for $K \lesssim 250$ MeV/c and demonstrates, that 3N interaction does not manifest itself within this region. At higher K the contribution of the 3N interaction becomes significant and from $K \sim 400$ MeV/c it dominates over the 2N interaction.

The contributions of different terms in Eq. (10) to the total momentum distribution are displayed in Fig. 2. It is worthwhile to note, that contribution of the most important term, $(\phi_1)^2$, has a dip in the same region (near $K \sim 450$ MeV/c) where the similar dip appears in calculations without 3N interactions.

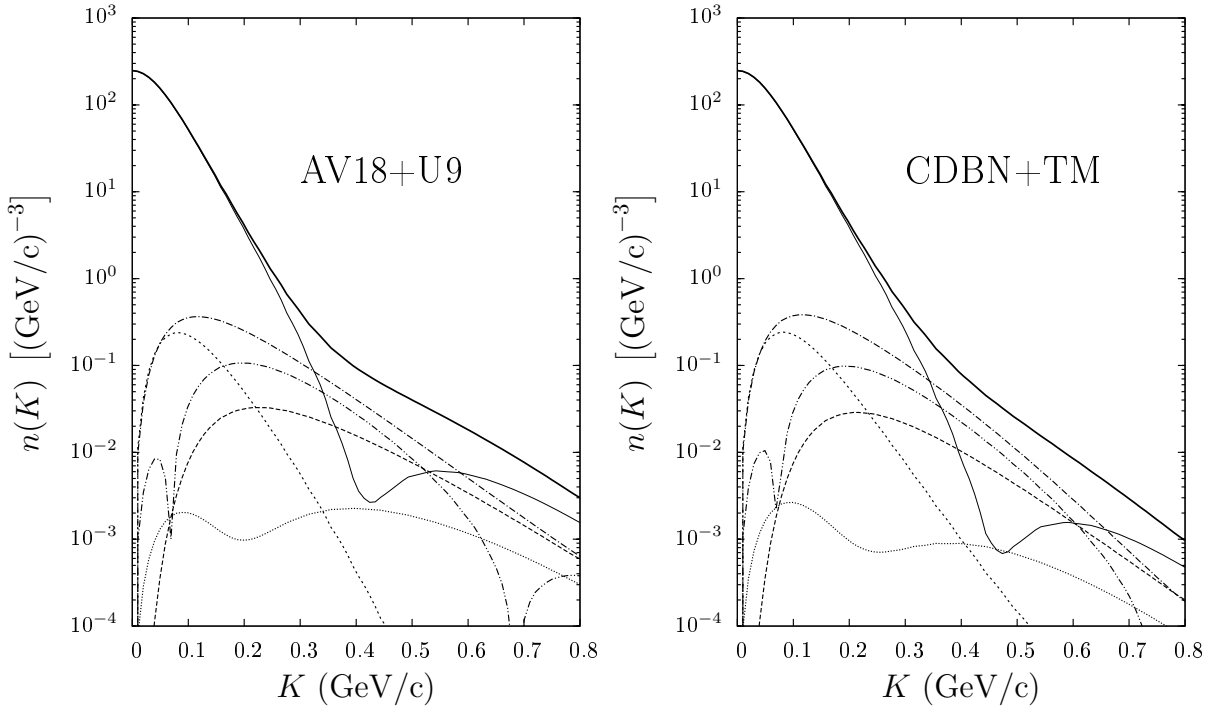

FIG. 2: Contribution of the main spin structures to the neutron momentum distribution in ^{3}He. Thin solid line: $(\phi_1)^2$; short dashed line: $(\phi_2)^2$; dotted line: $(\phi_6)^2$; long dashed line $(\phi_7)^2$; dot-dashed line: $(\phi_8)^2$; double-dot-dashed line: the absolute value of the sum of the interference terms $\phi_6\phi_7$, $\phi_6\phi_8$, and $\phi_7\phi_8$; bold solid line: the result with all the terms taken into account.

IV. MOMENTUM DISTRIBUTION OF PROTONS IN ^{3}HE

The momentum distribution of protons in ^{3}He is given by

$$n_p(K) = \tfrac{1}{2}\sum_\nu \int d^3p d^3q \left[\delta(\mathbf{p}_1 - \mathbf{K}) + \delta(\mathbf{p}_2 - \mathbf{K})\right] \times \left|\Psi_\nu(\mathbf{p},\mathbf{q})\right|^2 , \tag{11}$$

where $\mathbf{K}$ is the proton momentum in ^{3}He and the factor $\frac{1}{2}$ comes from averaging over the nucleus magnetic quantum numbers. Due to the identity of the protons, this expression is

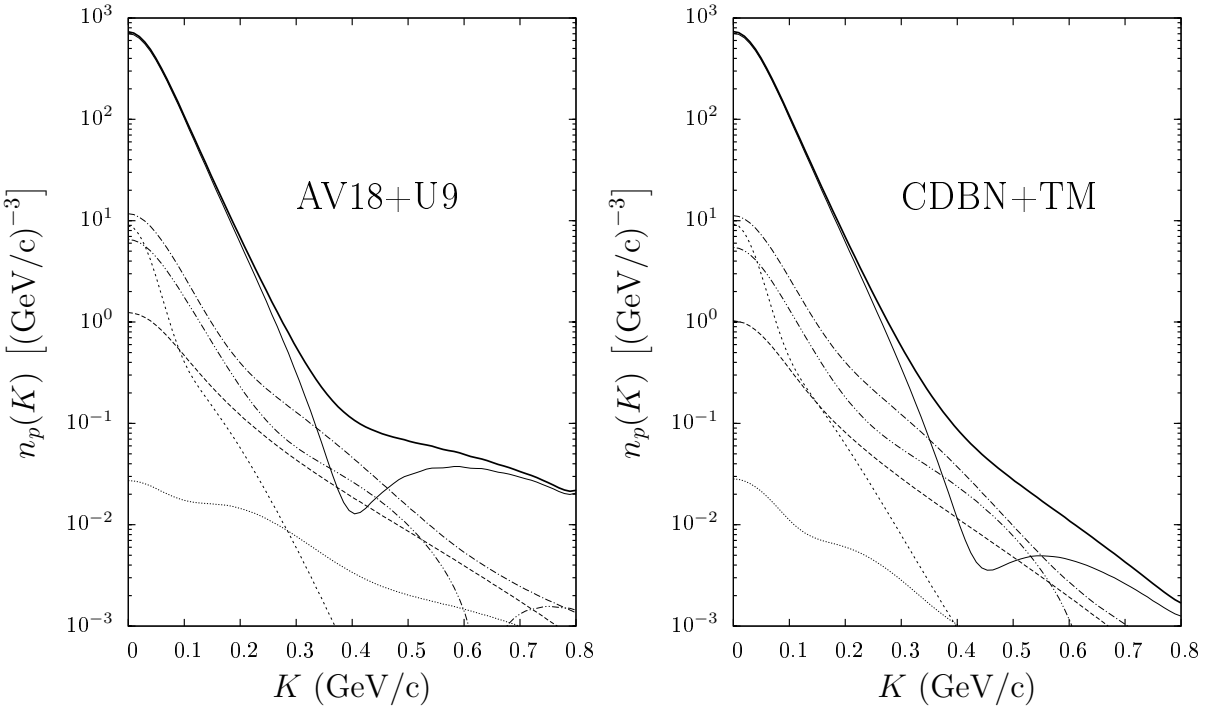

FIG. 3: Contribution of the main spin structures to the proton momentum distribution in ^{3}He. The notations are the same as those in Fig. 2.

reduced to

$$\begin{aligned} n_p(K) =& \sum_\nu \int d^3p d^3q \delta(\mathbf{p}_1 - \mathbf{K}) \left|\Psi_\nu(\mathbf{p},\mathbf{q})\right|^2 \\ \equiv& \sum_\nu \int d^3p d^3q \delta(\mathbf{p} - \tfrac{1}{2}\mathbf{q} - \mathbf{K}) \left|\Psi_\nu(\mathbf{p},\mathbf{q})\right|^2 \\ =& 2\int d^3p d^3q \delta(\mathbf{p} - \tfrac{1}{2}\mathbf{q} - \mathbf{K}) \Phi(p,q,x) \\ =& 32\pi \int_0^\infty dp p^2 \int_{-1}^1 d\cos\theta_p \Phi(p,q,x), \end{aligned} \tag{12}$$

where θ_p is angle between $\mathbf{p}$ and $\mathbf{K}$ and

$$\begin{aligned}\Phi(p,q,x) = &\left[C_{10}(p,q) + P_2(x)C_{12}(p,q)\right]^2 \\ &+ \left[P_1(x)C_{21}(p,q) + P_3(x)C_{23}(p,q)\right]^2 \\ &+ P_1^2(x)\left[C_{61}^2(p,q) + C_{71}^2(p,q)\right] \\ &+ \tfrac{9}{10}\left(1+\tfrac{1}{3}x^2\right)\left[C_{80}(p,q) + P_2(x)C_{82}(p,q)\right]^2 \\ &+ \left(-1+3x^2\right)P_1^2(x)C_{61}(p,q)C_{71}(p,q) \\ &+ \sqrt{\tfrac{24}{5}}xP_1(x)\left[C_{61}(p,q) + C_{71}(p,q)\right] \\ &\qquad \times \left[C_{80}(p,q) + P_2(x)C_{82}(p,q)\right].\end{aligned} \tag{13}$$

In the final line of Eq. (12), q and x are considered as functions of k, p, and θ_p. Using $\mathbf{K} = \mathbf{p} - \frac{1}{2}\mathbf{q}$, we get

$$\begin{aligned} q &= 2\sqrt{K^2 + p^2 - 2Kp\cos\theta_p}\,, \\ x &= \frac{p - K\cos\theta_p}{\sqrt{K^2 + p^2 - 2Kp\cos\theta_p}}. \end{aligned} \tag{14}$$

On the 2-dimensional grid, the integral over dp can be reduced to the sum $\sum_{i=1}^{n_p} w_i$, where w_i is an element on the grid (p,q,x). In turn, the integral over $d\cos\theta_p$ becomes

$$\int_{-1}^{1} d\cos\theta_p P_{\ell_1'}(x)P_n(\ell)C_{m\ell_1}(q,p_i)C_{m'\ell'}(q,p_i). \tag{15}$$

The variables x and q are defined by Eqs. (14) and thus q cannot be on the grid (p,q,x). Nevertheless, the functions $C_{m\ell_1}(q,p_i)$ and $C_{m'\ell'}(q,p_i)$ at fixed p_i, K, and $\cos\theta_p$ can be obtained by a linear interpolation from their values, given on the grid (q,p).

Contributions of the main spin structures, 1, 2, 6, 7, and 8 to the momentum distribution of protons in ^{3}He are displayed in Fig. 3.

V. EMPIRICAL MOMENTUM DISTRIBUTION

Here we compare the calculated proton momentum distributions with experimental results, extracted from the ^{12}C(^{3}He, p) breakup cross-section, measured at $p_{^3\mathrm{He}} = 10.8$ GeV/c with emission of the proton-fragments at 0° [1].

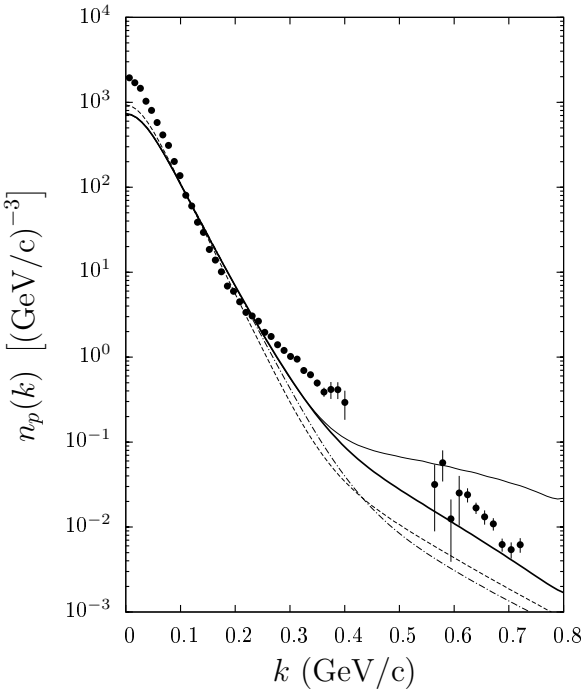

FIG. 4: The momentum distribution of protons in ^{3}He calculated with 2N+3N interaction. The notations of the curves are the same as those in Fig. 1. Circles represent the empirical momentum distribution extracted from the experimental data [1]. Here k is the LFD variable, as defined in Sect. V.

A. Empirical momentum distribution

To compare the calculated momentum distribution with experiment, it is necessary to establish a connection between the momentum $\mathbf{K}$ (which is a theoretical quantity) and the measured proton momentum. In the non-relativistic case it is of a common use to postulate that $\mathbf{K} = \mathbf{k}^*$, where $\mathbf{k}^*$ is the proton momentum is the ^{3}He rest frame. But in the relativistic case, as that of the experiment [1], it is incorrect.

The more adequate description has been suggested long time ago within the so-called "minimal relativization scheme". This approach was discussed in detail in Ref. [16], therefore here we remind only the main points.

In the framework of this scheme, the momentum $\mathbf{K}$ is to be identified with the "relativistic internal momentum" $\mathbf{k} = (\mathbf{k}_\perp, k_\parallel)$, which appears in the dynamics on the light front (LFD), instead of the non-relativistic $\mathbf{k}^*$. The LFD is often called as "dynamics in the infinite momentum frame" (IMF). (The IMF is defined as a limiting reference frame which is moving,

with respect to the laboratory frame, in the negative z-direction with velocity close to the speed of light.) In other words, it is $\mathbf{k}$ variable which corresponds to the variable $\mathbf{K}$, used in the previous sections. The important moment is: how the light-front variable $\mathbf{k}$ is related with the measurable momentum of a ^{3}He fragment?

In the IMF dynamics, the wave function of a bound state is described in terms of two variables, α and $\mathbf{k}_\perp$. Let us consider ^{3}He as a proton+2N system with masses m and $\mathcal{M}_{2N}$; then α and $\mathbf{k}_\perp$ are defined by

$$\alpha = \frac{E_p^{\rm lab} + k_\parallel^{\rm lab}}{E_{^3{\rm He}}^{\rm lab} + P_\parallel^{\rm lab}}, \qquad \mathbf{k}_\perp = k_\perp^{\rm lab}, \tag{16}$$

where $p = (E_p^{\rm lab}, \mathbf{k}_\perp^{\rm lab}, k_\parallel^{\rm lab})$ and $P = (E_{^3{\rm He}}^{\rm lab}, \mathbf{0}_\perp, P^{\rm lab})$ are the proton and ^{3}He 4-momenta in the laboratory frame. In terms of α and $\mathbf{k}_\perp$, the effective mass squared of (p+2N) system becomes

$$\mathcal{M}^2_{p+2{\rm N}} = \frac{\alpha m^2 + (1-\alpha)\mathcal{M}^2_{2{\rm N}} + \mathbf{k}_\perp^2}{\alpha(1-\alpha)} \tag{17}$$

and the longitudinal component of the $\mathbf{k}$ momentum is given by

$$k_\parallel = \pm\sqrt{\frac{\lambda(\mathcal{M}^2_{3{\rm N}}, \mathcal{M}^2_{2{\rm N}}, m^2)}{4\mathcal{M}^2_{3{\rm N}}} - \mathbf{k}_\perp^2}, \tag{18}$$

where $\lambda(a,b,c) = a^2 + b^2 + c^2 - 2ab - 2ac - 2bc$. In Ref. [16] it was argued that, because the mean momentum square in the pair $\langle q^2\rangle \ll m^2$, one can take $\mathcal{M}_{2{\rm N}} \approx 2m$.

From the kinematical conditions of experiment [1] it follows, that $\mathbf{q}_\perp = 0$ and $\mathbf{k}_\perp = 0$. In this case the signs " $-$ " and " $+$ " are chosen for $\alpha < \frac{1}{3}$ and $\alpha > \frac{1}{3}$, respectively; the IMF momentum $\mathbf{k}$ is reduced to the momentum $\mathbf{k}^*$ for $\alpha \approx \frac{1}{3}$.

The integral

$$\begin{aligned} &\int d^3k n_p(k) \\ &= \int_0^1 d\alpha \int d^2k_\perp \frac{\varepsilon_p(k)\varepsilon_p(k)}{\alpha(1-\alpha)\mathcal{M}_{3{\rm N}}} n_p(k) = 2, \\ &\varepsilon_p(k) = \sqrt{m^2 + k^2}, \qquad \varepsilon_{2N}(k) = \sqrt{M^2 + k^2} \end{aligned} \tag{19}$$

gives number of protons in ^{3}He and the following expression can be considered as the relativized momentum distribution of protons in ^{3}He:

$$n_p^{\rm rel}(\alpha, \mathbf{k}_\perp) = \frac{\varepsilon_p(k)\varepsilon_d(k)}{\alpha(1-\alpha)\mathcal{M}_{3{\rm N}}} n_p(k). \tag{20}$$

After that, in the framework of IMF dynamics, the invariant differential cross-section of the $A(^3\mathrm{He}, p)$ breakup is given by

$$
\begin{aligned}
E_p \frac{d^3\sigma}{d\mathbf{p}_p} &= f_{\mathrm{kin}}^{(p)} \sigma_d (1-\alpha) n_p^{\mathrm{rel}}(\alpha, \mathbf{k}_\perp), \\
f_{\mathrm{kin}}^{(p)} &= \frac{\lambda^{\frac{1}{2}}(W, m^2, M_A^2)}{2\alpha M_A P},
\end{aligned}
\tag{21}
$$

where W and M_A are the missing mass squared and the mass of the target nucleus, respectively; the σ_d factor plays a role of normalization factors.

Eq. (21) can be used to extract the proton momentum distribution in ^{3}He.

It is clear that this equation was derived in the framework of the impulse approximation. Nevertheless, one may expect that the momentum distribution extracted from experimental data effectively includes effects beyond the impulse approximation, in particular, coming from the quark structure of ^{3}He. Therefore it was called in Ref. [16] as "empirical momentum distributions" (EMD) of the protons in ^{3}He.

B. Comparison with experiment

In Fig. 4 we compare results of our calculations for EMD extracted from data [1], as well as with the calculations of Ref. [16], based on 2N interactions only.

There is rather good agreement between calculations and EMD data at $k \lesssim 250$ MeV/c. At very small k ($\lesssim 50$ MeV/c) an enhancement of EMD data over theoretical curves is obvious as for the ^{3}He case, as for the deuteron case. This effect can be naturally explained as a result of contributions of the Coulomb interaction to the breakup with registration of a charged fragment at zero emission angle. It should be noted, that similar enhancement takes place also in EMD of protons in the deuteron, extracted from data on the $^{12}\mathrm{C}(d, p)$ breakup [19]. Calculations published in Ref. [20], based on the Glauber-Sitenko model, support interpretation of this enhancement as a manifestation of the Coulomb interaction.

From comparison of our results with the EMD data under discussion and with results published in Ref. [16] at $k > 250$ MeV/c, the following conclusions can be drawn:

- There is rather visible qualitative disagreement between calculations and EMD of protons in ^{3}He.

- Contribution of 3N interactions becomes significant in $k > 250$ MeV/c region, but cannot explain completely the disagreement between the data on EMD of protons and calculations, based on 2N interactions only.

- Version of the ^{3}He wave function based on the CDBN+TM potential looks more preferable than the version, based on the AV18+U9 potential, because the latter one strongly overestimates the EMD data at very high momenta (above 600 MeV/c).

VI. CONCLUSIONS

The momentum distributions of neutrons and protons in ^{3}He have been calculated using the so-called "operator" form for description of the 3N system. We used results of Ref. [10], where calculations of the necessary scalar functions (appearing in the operator form representation of the bound 3N system) were performed with two potentials, which take into account effective 3N interactions, the 2N interaction AV18 [11] with the interaction Urbana-IX [12] (AV18+U9) and the 2N interaction CD-Bonn [13] with insertion of the 3N Tucson-Melbourne interaction [14] (CDBN+TM).

We compare our results with calculations of Ref. [16] which do not take into account the 3N interaction and conclude, that 3N interactions become essential at the large internal momentum $K >$250 MeV/c of a nucleon in the bound 3N system.

We also compare the calculated momentum distribution of protons with the so-called empirical momentum distribution in ^{3}He, extracted from $(^3\mathrm{He}, p)$ breakup cross-section [19], and conclude, that 3N interactions reduce disagreement between theory and experiment at $k >$250 MeV/c. Nevertheless, this disagreement does not completely disappear even in the case when the 3N interactions are taken into account.

That means, that non-nucleon degrees of freedom in ^{3}He, as well as mechanisms beyond the so-called " impulse approximation", become important in the ^{3}He breakup at $k >$250 MeV/c and all other processes, where the nucleon-constituents of this nucleus (as well as other nuclei) are very close (at distances <0.8 fm) to each other.

---

[1] V.G. Ableev et al., JETP Lett. **45**, 596 (1987); Pis'ma v ZhETP **45**, 467 (1987).

[2] V. Baru, J. Haidenbauer, C. Hanhart, and J.A. Niskanen, Eur. Phys. J. **A 16** 437 (2003).

[3] V.V. Kotlyar and A.V. Shebeko, Zeitschrift für Physik A**327**, 301 (1987).

[4] V.V. Kotlyar and A.A,Scsheglova, Visnyk Khrkivs'kogo univerytetu, No832, seria "physics", v. 4(40) (2000) (on Russian).

[5] V.V. Kotlyar and J. Jourdan, Problems of Atomic Science and Thechnology. Series: Nucl. Phys. Investigations **6(45)**, 24 (2005).

[6] E. Gerjouy and J. Schwinger, Phys. Rev. **61**, 138 (1942).

[7] W. Rarita and J. Schwinger, Phys. Rev. **59**, 436 (1941); Phys. Rev. **59**, 556 (1941).

[8] I.V. Simenog, I.S. Dotsenko, and B.E. Grinyuk, Ukr. J. Phys. bf 47, 129 (2002).

[9] I.S. Dotsenko and I.V. Simenog, Ukr. J. Phys. bf 51, 841 (2002).

[10] I. Fachruddin, W. Glökle, Ch. Elster, and A. Nogga, Phys. Rev. C **69**, 064002 (2004).

[11] R.B. Wiringa, V.G.T. Stoks, and R. Schiavilla, Phys. Rev. C **51**, 35 (1995).

[12] B.S. Pudler et al., Phys. Rev. C **56**, 1720 (1997).

[13] R. Machleidt, Phys. Rev. C **63**, 024001 (2001).

[14] S.A. Coon et al., Nucl. Phys. A **317**, 242 (1972); S.A. Coon and W. Glöckle, Phys. Rev. C **23**, 1790 (1981).

[15] http://www.phy.ohiou.edu/∼elster/h3wave/

[16] A.P. Kobushkin and E.A. Strokovsky, Phys. Rev. C **87**, 024002 (2013).

[17] R. Schiavilla, V.P. Pandripanda, and R.B. Wiringa, Nucl. Phys. **A449**, 219 (1986).

[18] M. Lacombe et al., Phys. Rev. **C 21**, 861 (1980).

[19] V.G. Ableev et al., Nucl. Phys. **A 393** 491 (1983) and **A 411** 541 (E) (1983); V.G. Ableev et al., JINR Rapid Comm. 1[52]-92 10 (1992); V.G. Ableev et al., JINR Rapid Comm. 1[52]-92 5 (1992) and Phys. Atom. Nucl. **37**, 132 (1983).

[20] A.P. Kobushkin and Ya.D. Krivenko-Emetov, Ukr. J. Phys. **53**, 751 (2008).